doi:10.1038/nature11079

Supplementary Figures

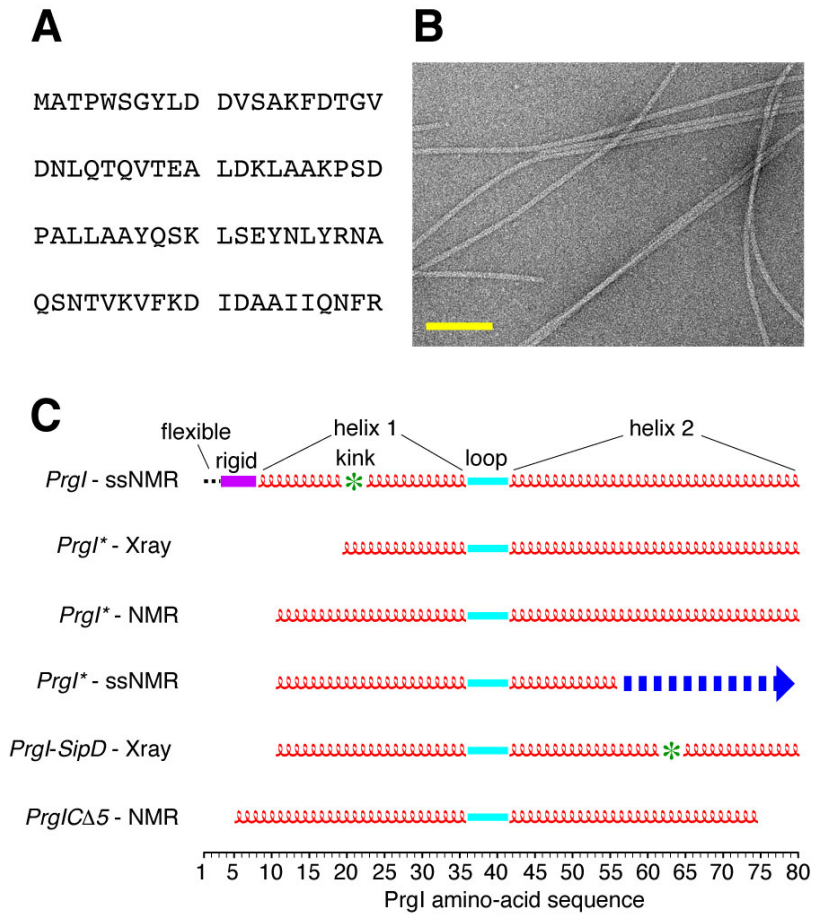

Supplementary figure 1. (A) Amino-acid sequence of the wild-type *S. typhimurium* PrgI subunit in one-letter code. (B) Electron micrograph of PrgI needles (Scale bar: 100 nm), used for ssNMR experiments. (C) Comparison of the secondary structure elements for different PrgI structures: the wild-type filamentous needle assembly presented here (PrgI - ssNMR), the crystal structure of double-mutant (V65A/V67A) PrgI*[1] (PrgI* - X-ray), the structure of soluble double-mutant (V65A/V67A) PrgI* analyzed by solution NMR[1] (PrgI* - NMR), the model of the double-mutant (V65A/V67A) PrgI* in the needle assembly[1] (PrgI* - ssNMR), the crystal structure of double-mutant (V65A/V67A) PrgI* together with the tip protein SipD[2] (PrgI-SipD – X-ray), and the solution structure of C-terminally truncated PrgI analyzed by solution NMR[3] (PrgICΔ5 – NMR). Disordered regions are not depicted.

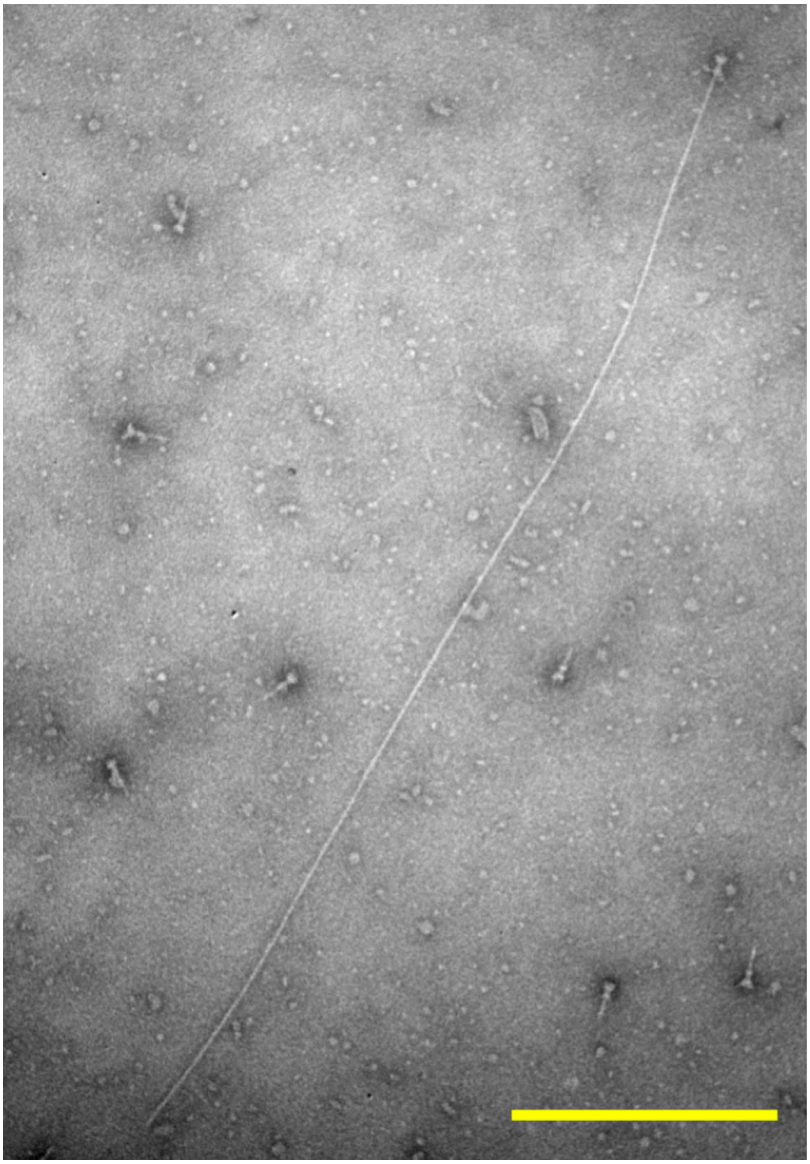

Supplementary figure 2. Electron micrograph of *S. typhimurium* T3SS needle elongated with purified wild-type PrgI protomers (Scale bar: 500 nm).

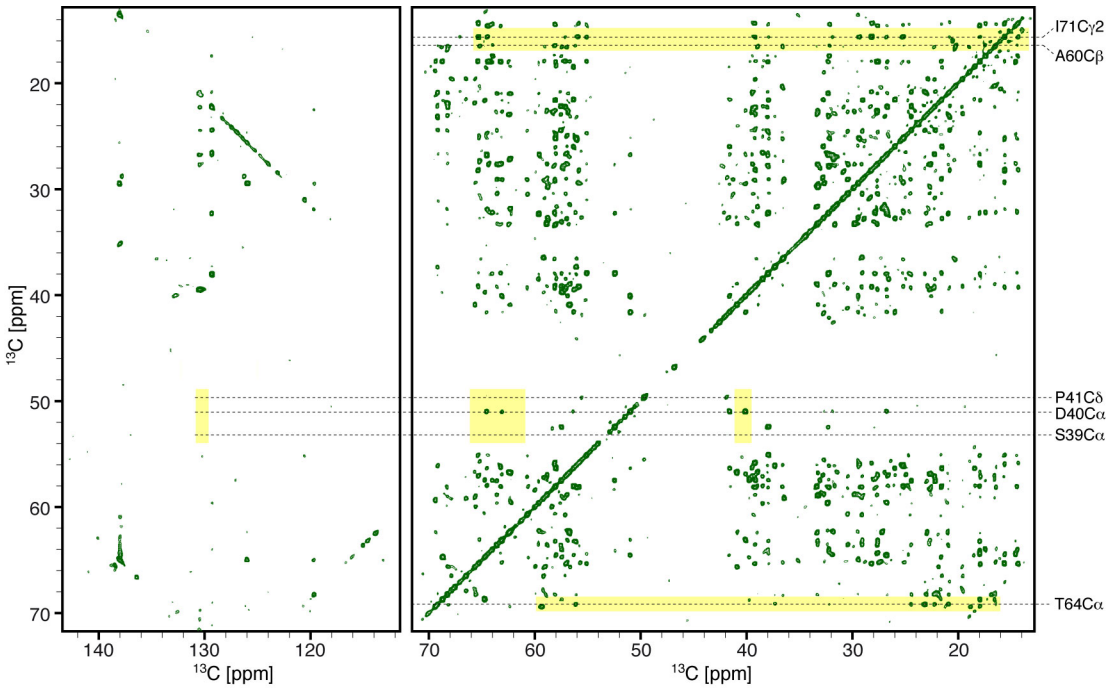

Supplementary figure 3. 2D ^{13}C-^{13}C correlation spectrum of [1-^{13}C]-Glc-labeled T3SS needles (recorded at 20.0 Tesla with a mixing time of 850 ms). The excerpts shown in main text Fig. 1 are highlighted in yellow.

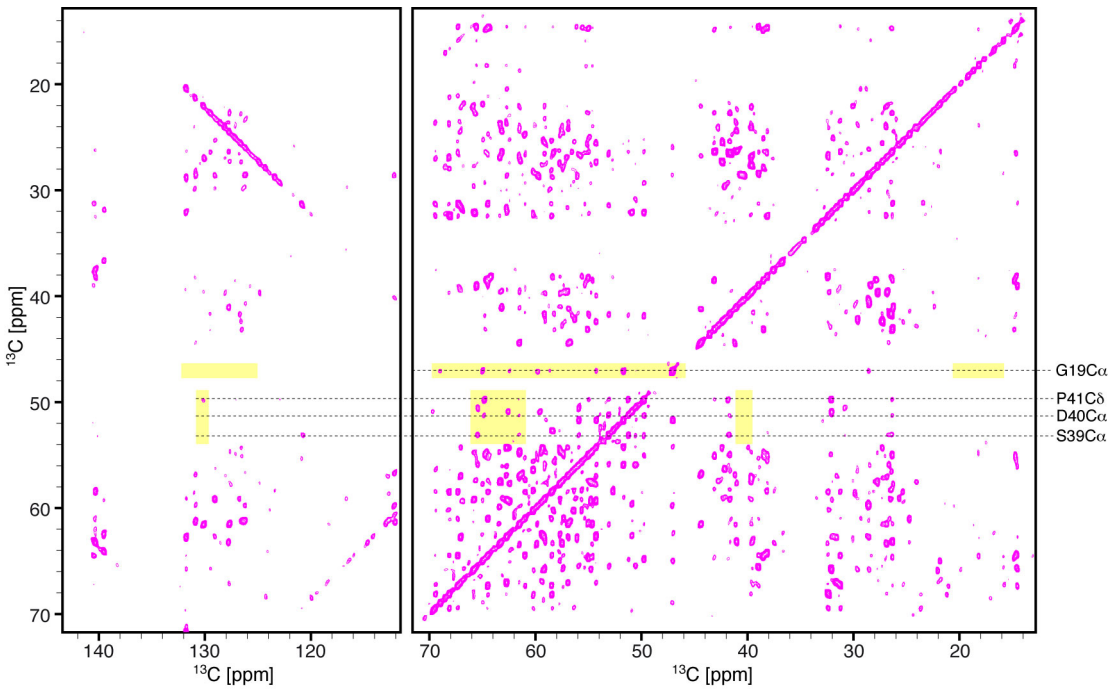

Supplementary figure 4. 2D ^{13}C-^{13}C correlation spectrum of [2-^{13}C]-Glc-labeled T3SS needles (recorded at 20.0 Tesla with a mixing time of 850 ms). The excerpts shown in main text Fig. 1 are highlighted in yellow.

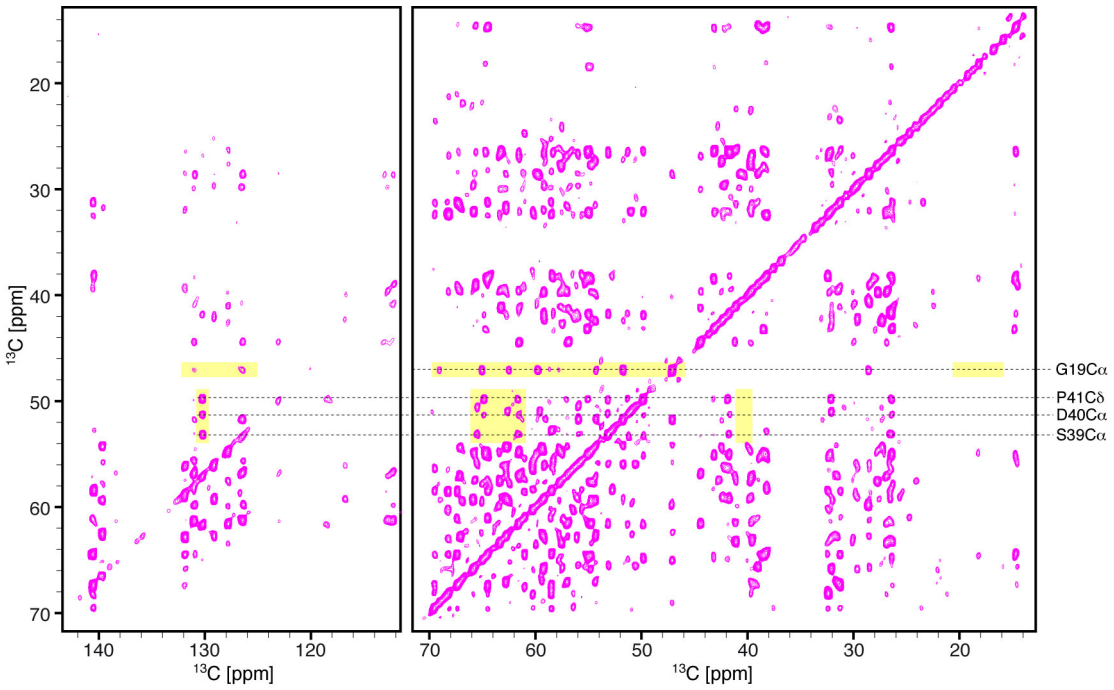

Supplementary figure 5. 2D ^{13}C-^{13}C correlation spectrum of [2-^{13}C]-Glc-labeled T3SS needles (recorded at 14.1 Tesla with a mixing time of 1000 ms). The excerpts shown in main text Fig. 1 are highlighted in yellow.

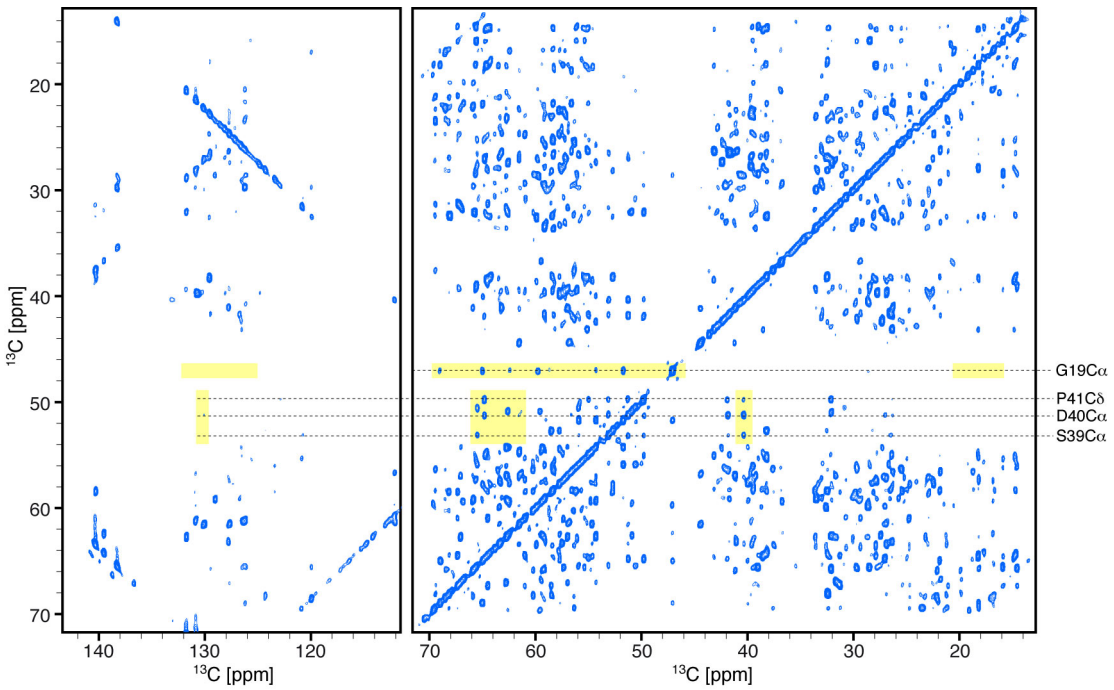

Supplementary figure 6. 2D ^{13}C-^{13}C correlation spectrum of [(1/2)-^{13}C]-Glc-labeled T3SS needles (recorded at 20.0 Tesla with a mixing time of 850 ms). The excerpts shown in main text Fig. 1 are highlighted in yellow.

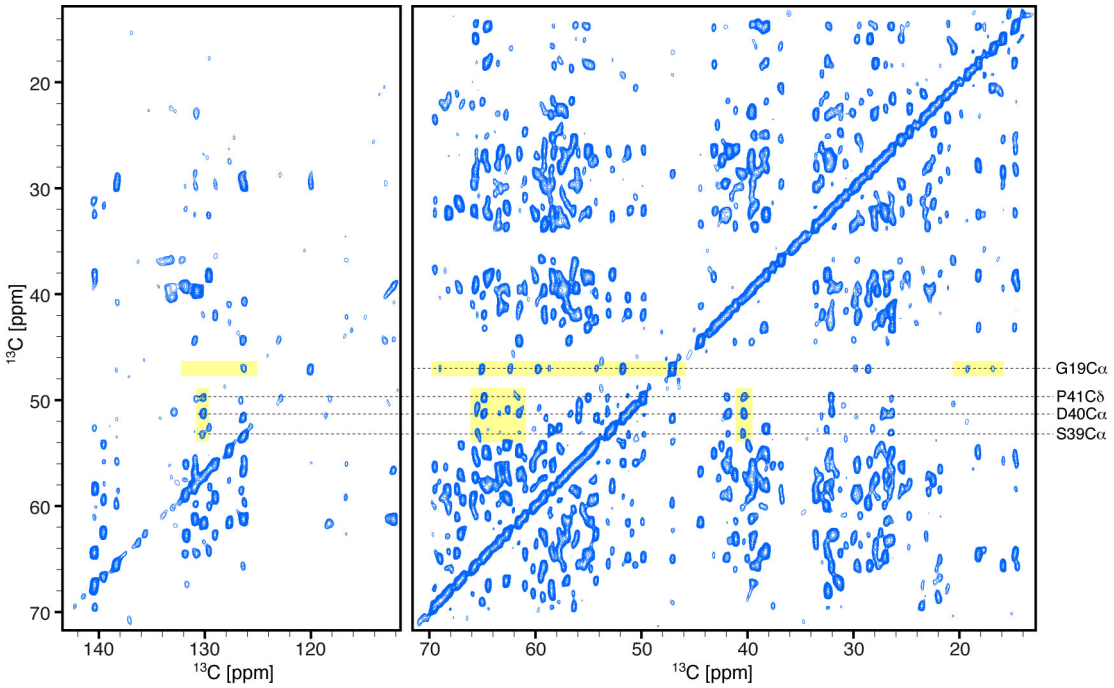

Supplementary figure 7. 2D ^{13}C-^{13}C correlation spectrum of [(1/2)-^{13}C]-Glc-labeled T3SS needles (recorded at 14.1 Tesla with a mixing time of 1000 ms). The excerpts shown in main text Fig. 1 are highlighted in yellow.

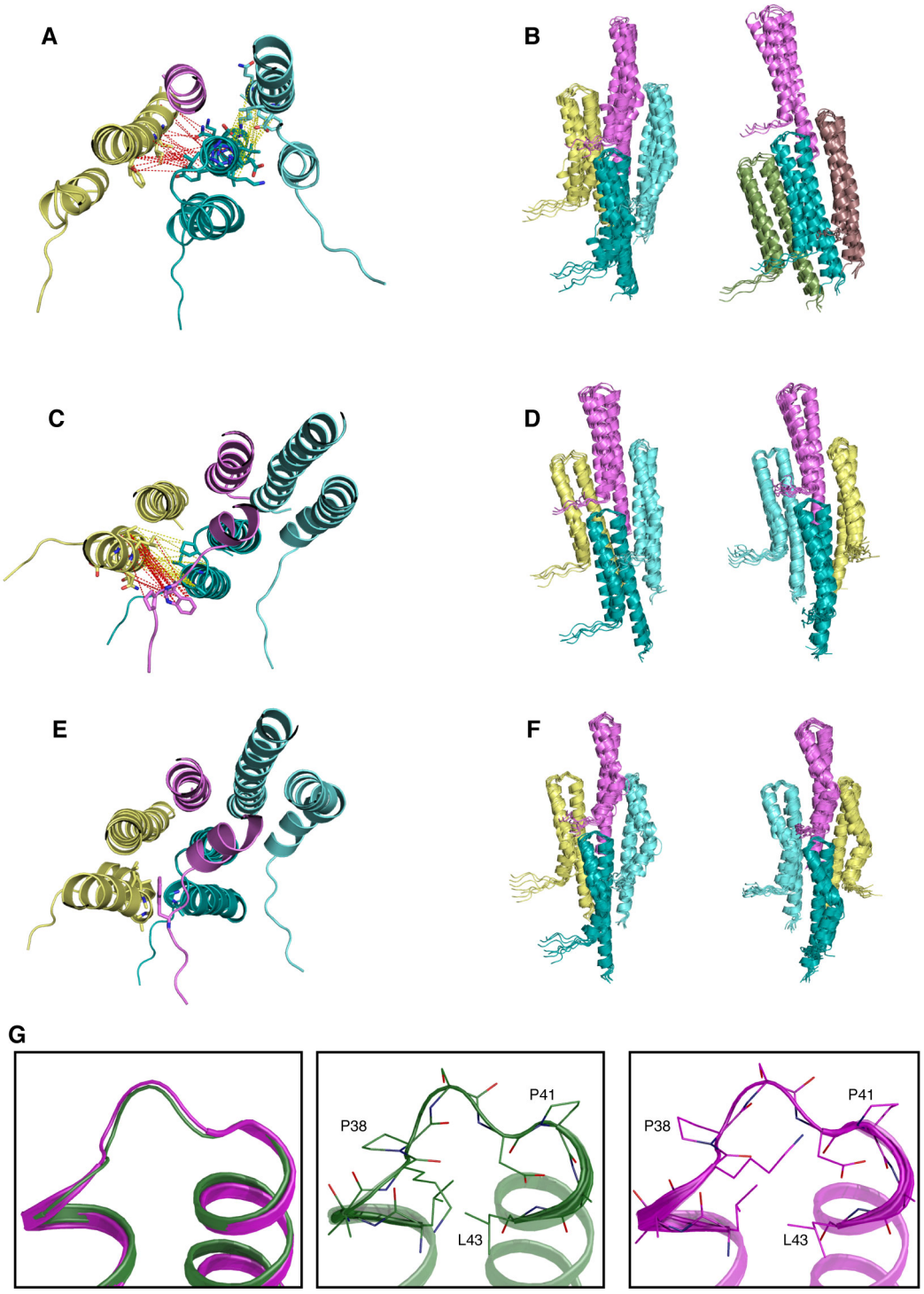

Supplementary figure 8. Overview of the needle model determination process. Low-energy ensembles of increasing convergence are shown at different restraint assignment stages. The assignments of restraint clusters are indicated with dashed lines at different stages of the structure determination process on the left top views. Yellow dashed lines indicate restraints that are used during the current calculation stage, while red dashed

lines indicate newly identified restraints. Calculations were carried out assuming an 11-start helix and, in addition to the intra-molecular restraints, (A, B) unambiguous axial restraints only (C, D) axial and lateral inner-helical restraints (E, F) after assignment of the outer-helical interactions using all identified inter-subunit restraints. For clarity, only four contacting subunits are shown: i (blue), i+5 (cyan), i+6 (yellow), and i+11 (magenta). In (B, D, F) left-handed models are shown on the left while right-handed models on the right. In (B) the i-1 and i+1 subunits are shown as green and red, respectively. The overall topology of the needle is well defined using all the data without resolving (5/6)-ambiguities (A) but key side chain interactions only become well defined after resolution of the (5/6)-ambiguities (E). (G) Comparison of the central region of PrgI (L34-L43) between the atomic model presented in this work (in green) and the crystal structure of the double-mutant (V65A/V67A) PrgI* (in magenta).

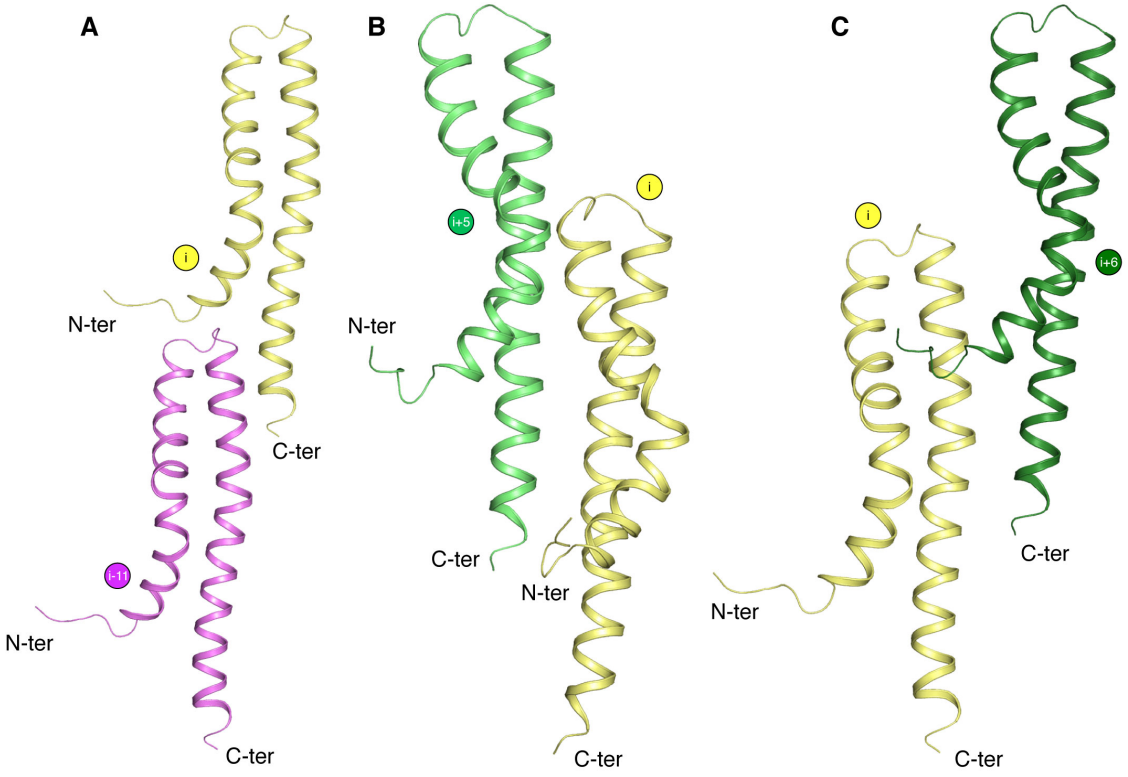

Supplementary figure 9. Overview of the different supramolecular interfaces in the T3SS needle.

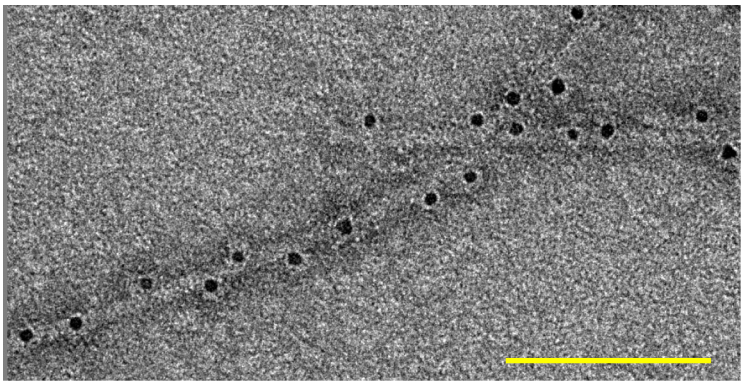

Supplementary figure 10. Electron micrograph of *S. typhimurium* T3SS needles formed from an N-terminal His-tag fusion construct of PrgI, incubated with an Anti-His-tag monoclonal antibody (Scale bar: 100 nm).

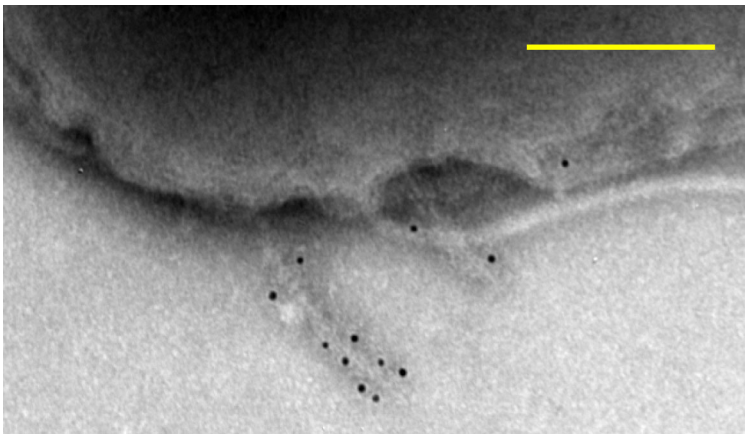

Supplementary figure 11. Electron micrograph of a *S. typhimurium prgI-knockout* cell complemented with *prgI* fused to an upstream Strep-tag II, labeled with anti-Strep antibodies (Scale bar: 200 nm).

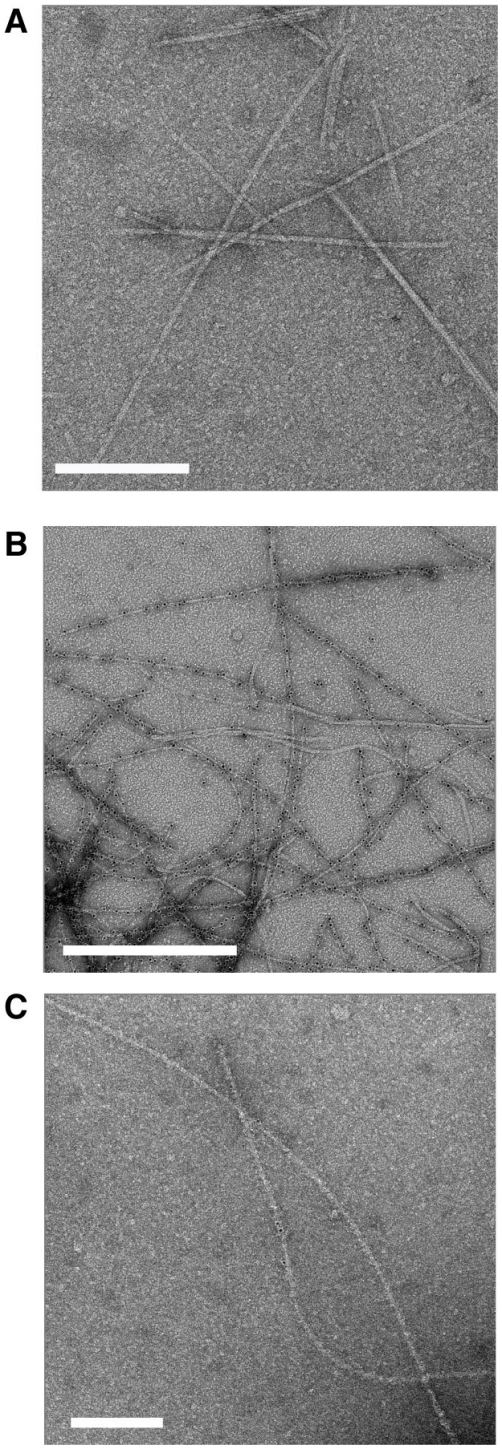

Supplementary figure 12. Immunogold-labeling of *S. typhimurium* T3SS needle using an Anti-His-tag monoclonal antibody (Invitrogen). The labeling was performed using a 1:200 diluted antibody and 10 nm protein A Gold (Posthuma, Utrecht) (A) wild-type needles (Scale bar: 200 nm). (B) N-terminal His-tag fusion construct needles (Scale bar: 500 nm). (C) N-terminal His-tag fusion construct needles labeled without primary antibody (Scale bar: 200 nm).

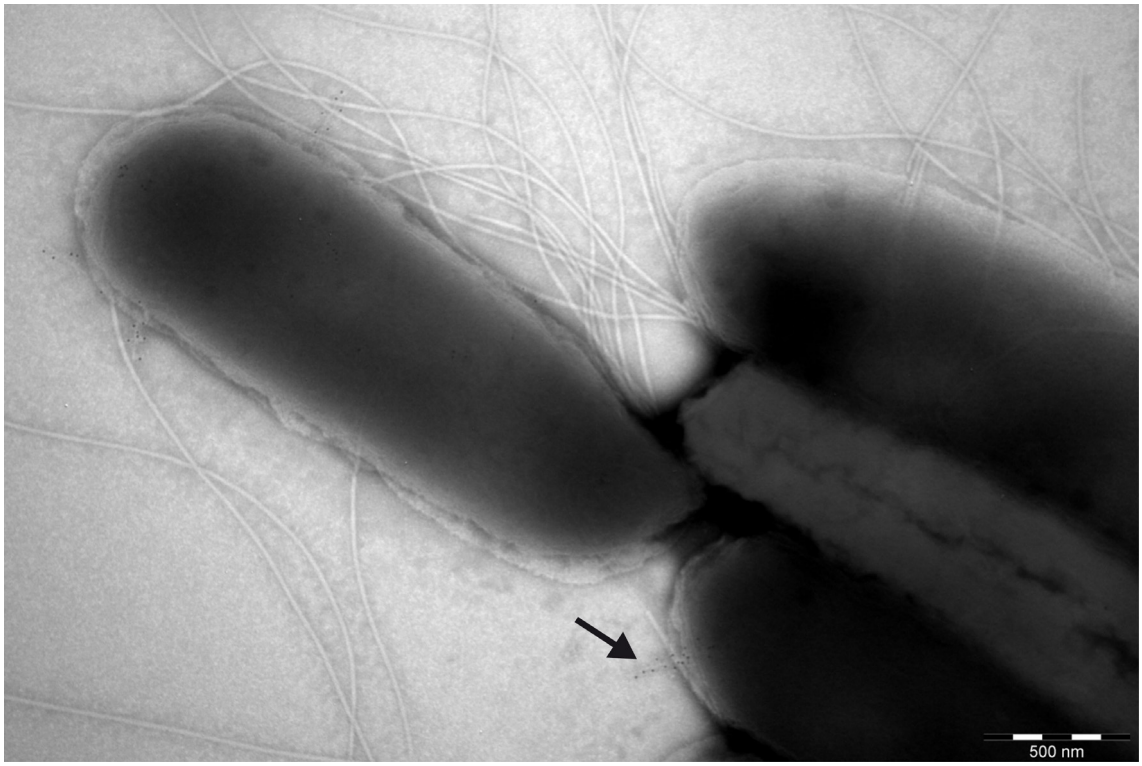

Supplementary figure 13. Electron micrograph of *S. typhimurium prgI-knockout* cells complemented with *prgI* fused to an upstream Strep-tag II, labeled with anti-Strep antibodies (Scale bar: 500 nm). The arrow indicates a T3SS needle.

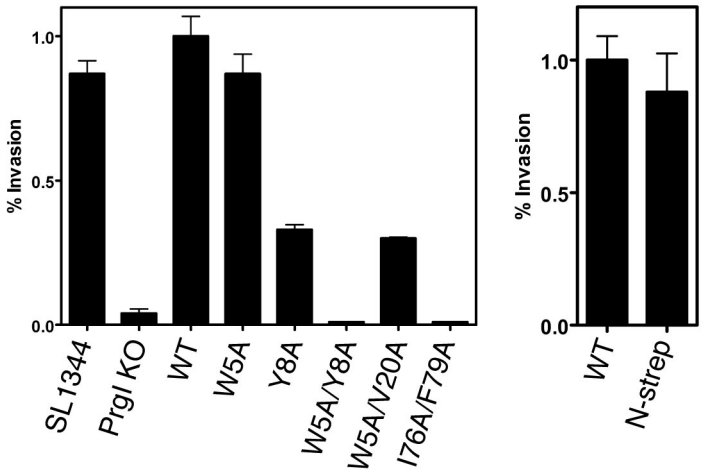

Supplementary figure 14. Invasiveness of several PrgI mutants. Error bars, s.d. (n = 3).

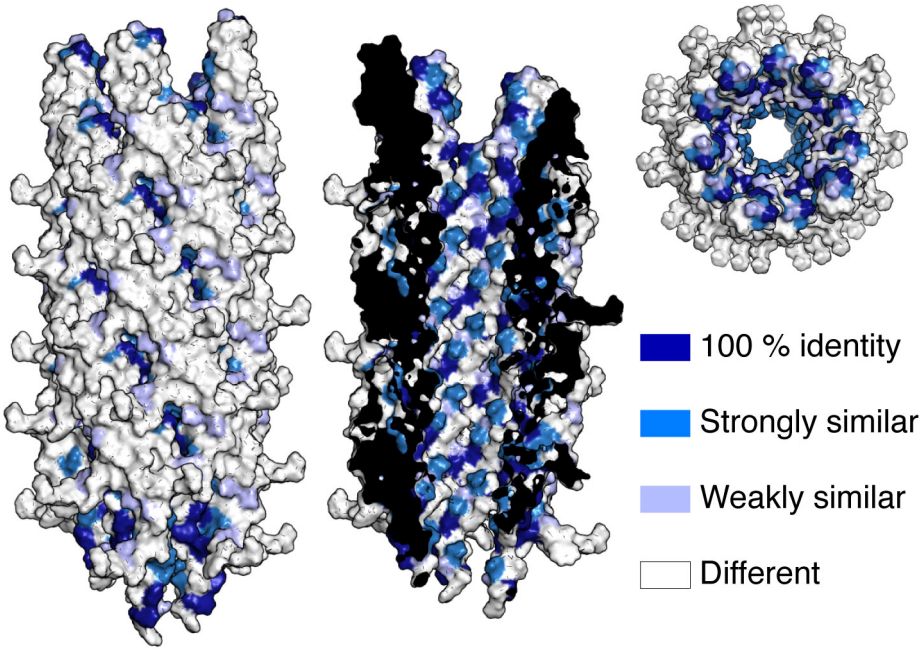

Supplementary figure 15. Surface representation of the T3SS needle, showing the conservation of the residues between different bacterial species. The front of the needle is cut away in the middle panel to reveal the interior of the channel.

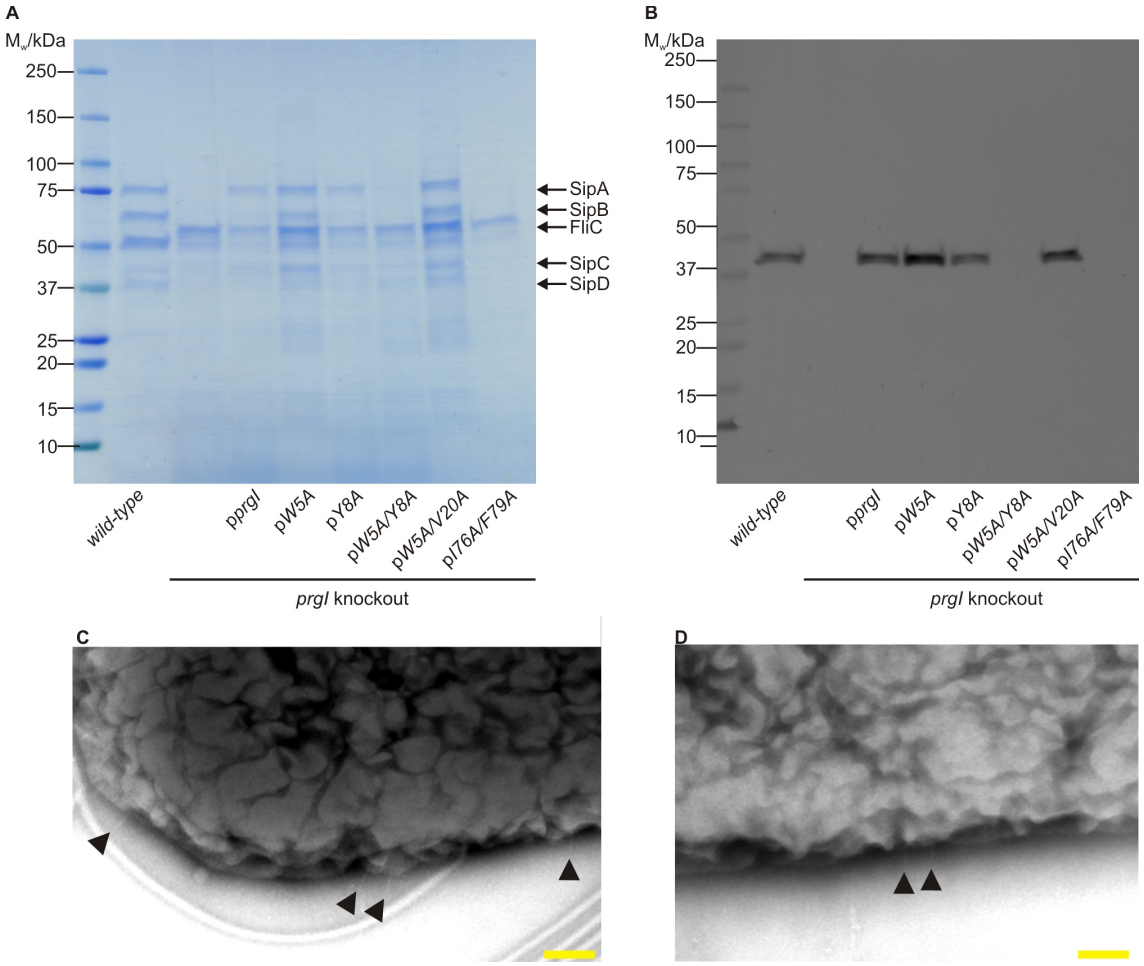

Supplementary figure 16. (A) Protein secretion assay of wild-type and *prgI knockout* *S. typhimurium* complemented with either p*prgI* or mutated *prgI* (p*W5A*, p*Y8A*, p*W5A*/*Y8A*, p*W5A*/*V20A*, and p*I76A*/*F79A*), see also[4] for effector secretion (B) Western blot of SipC secreted from *S. typhimurium* strains as in (A). Electron micrograph of *S. typhimurium* (C) and p*prgI* complemented *knockout* cells (D), arrows indicate T3SSs (Scale bar: 100 nm).

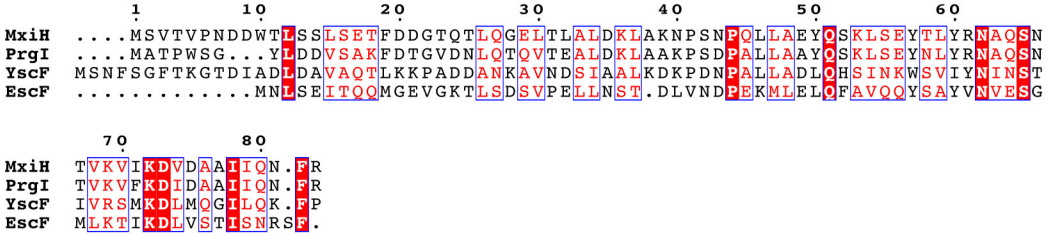

Supplementary figure 17. Sequence alignment for needle proteins from *Shigella flexneri* (MxiH), *Salmonella typhimurium* (PrgI), *Yersinia pestis* (YscF), and *Escherichia coli* (EscF).

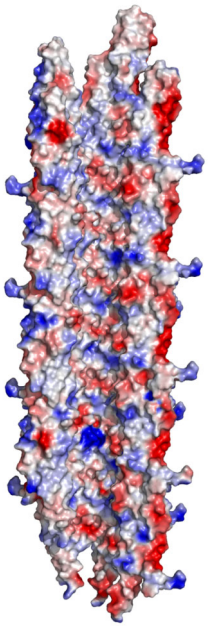

Supplementary figure 18. Electrostatic potential of the PrgI channel surface. The Poisson-Boltzmann potential was calculated and mapped onto the molecular surface of the PrgI channel. The computational results for the electrostatic surface were obtained using DelPhi[5] and the graphic display was produced using Pymol [6].

Supplementary Tables

Type of distance restraints	Total	[1-^{13}C]-Glc	[2-^{13}C]-Glc	[(1/2)-^{13}C]-Glc
Total	521	227	244	50
Medium-range ($2 \leq |i-j| \leq 4$)	274	116	157	1
Intra-subunit long-range ($|i-j| > 4$)	85	48	34	3
Inter-subunit long-range	162	63	53	46

Supplementary table 1. Number of ssNMR distance restraints used for the determination of the T3SS needle model.

	Restraints****	Subunits/Turn	Rise/subunit	RMSD**	N.O.R.*	***Energy
Stage I	Axial only	5.20-5.76/10.4-11.85	3.99-4.40A	3.5A	413	-155 / -176
Stage IIR	Axial+lateral(R)	5.61-5.76	4.06-4.32A	2.5A	464	-177
Stage IIL	Axial+lateral(L)	5.58-5.80	4.11-4.34A	2.5A	464	-174
Stage IIIR	Axial+lateralB(R)	5.56-5.66	4.08-4.35A	2.1A	512	-166
Stage IIIL	Axial+lateralB(L)	5.58-5.68	4.20-4.40A	2.3A	512	-150

*N.O.R. number of restraints used in each calculation stage.
**RMSD values are reported within the backbone of each low-energy cluster as a metric of convergence.
***Full atom interface energy in Rosetta energy units.
**** Intra-subunit restraints were included in all calculations.

Supplementary table 2. Summary of calculation details and structure statistics at different calculation stages.

Type	Rise(Å)	Monomers/turn	N-terminus	Restr. Energy
9-start	4.6-5.0	4.5-4.6	Outside	81-115
11-start	4.0-4.4	5.5-5.7	Outside	77-92
13-start	3.5-3.8	6.4-6.7	Outside	81-104
15-start	2.9-3.3	7.4-7.7	Outside	89-99

Supplementary table 3. Summary of calculation results for individual helix geometries. Both right-and left-handed geometries were considered in each case.

1 Poyraz, O. *et al.* Protein refolding is required for assembly of the type three secretion needle. *Nat. Struct. Mol. Biol.* **17**, 788-792, (2010).
2 Lunelli, M., Hurwitz, R., Lambers, J. & Kolbe, M. Crystal structure of PrgI-SipD: insight into a secretion competent state of the type three secretion system needle tip and its interaction with host ligands. *PLoS Pathog* **7**, e1002163, (2011).
3 Wang, Y. *et al.* Differences in the electrostatic surfaces of the type III secretion needle proteins PrgI, BsaL, and MxiH. *J Mol Biol* **371**, 1304-1314, (2007).
4 Kimbrough, T. G. & Miller, S. I. Contribution of Salmonella typhimurium type III secretion components to needle complex formation. *Proc Natl Acad Sci U S A* **97**, 11008-11013, (2000).
5 Honig, B. & Nicholls, A. Classical electrostatics in biology and chemistry. *Science* **268**, 1144-1149, (1995).
6 DeLano, W. L. PyMOL. www.pymol.org, (2005).